Korean J. Chem. Eng., **30**(7), 1423-1428 (2013)
DOI: 10.1007/s11814-013-0074-z

Detection of reactive oxygen species generated by microwave electrodeless discharge lamp and application in photodegradation of H_2S

Yang Yu, Tingting Zhang, Liqiong Zheng, and Jiang Yu†

College of Chemical Engineering, Beijing University of Chemical Technology, Beijing 100029, P. R. China
(*Received 30 December 2012 • accepted 4 May 2013*)

Abstract−The photodegradation of hydrogen sulfide (H_2S) was examined using a self-made microwave electrodeless discharge lamp (MEDL). The features of the MEDL had been tested. The results showed that the MEDL absorbed 18.3, 32.7 and 41.8 W power at the microwave (MW) output power of 165, 330 and 660 W, respectively. The intensity of the emitted light increased with increasing MW output power. The reactive oxygen species (ROS) generated by irradiated air and nitrogen were detected, respectively. It was illustrated that the irradiated air could generate a number of ROS, at least including $^1O_2$ and •OH. And the amount of ROS increased with increasing MW output power. In photodegradation of H_2S process, the effects of MW output power and gas composition were investigated. The removal efficiency of H_2S under nitrogen was obviously lower compared with that under air. The removal efficiency of H_2S increased with increasing MW output power.

Key words: Microwave Electrodeless Discharge Lamp (MEDL), Reactive Oxygen Species (ROS), Photodegradation, Hydrogen Sulfide

INTRODUCTION

Hydrogen sulfide (H_2S) is a representative odorous pollutant released as a by-product of many processes, such as sour gas flaring, petroleum refining, pulp and paper manufacturing or wastewater treatment [1-3]. H_2S has an extremely low odor threshold (0.5 ppb) [4]; not only it can cause corrosion of expensive metal parts, but also can threaten human safety [5,6]. Therefore, a cost-effective technology for treatment of reduced H_2S is highly desired.

Many studies have been conducted on the photocatalytic oxidation of H_2S at low concentration using TiO_2 [7-9]. Compared to other techniques, the photocatalytic oxidation of H_2S offers several advantages, such as low cost, energy saving and minimal waste. However, very few commercial applications of this technology are available at present due to deactivation of the catalyst and low quantum efficiency. During the course of the photocatalytic reaction, the by-products and products accumulated on the surface of TiO_2 could cause the deactivation of the catalyst [7,10]. Most of the photoinduced positive holes (h^+) and electrons (e^-) had recombined before they were trapped by hydroxyl or oxygen and quantum efficiency was usually less than 5% [11].

To enhance the quantum efficiency of the photocatalytic oxidation, microwave (MW) energy was used to assist photocatalytic reactions for MW radiation could somehow affect the activity of the TiO_2 particle surface. In this context, microwave electrodeless discharge lamp (MEDL) has been used in many photocatalytic processes as illuminant [12-15]. When placed into the MW field, the MEDL will generate UV-Vis radiation by absorbing the MW power. And at the same time, the MW field interacts with the reaction mixture [16,17]. Therefore, the application of MEDL brings the simultaneous effect of both UV-Vis and MW irradiations on photochemical reactions. At present, this technique is mainly used to photo oxidize organic pollutants in aqueous solution. Nevertheless, the photodegradation of inorganic compounds in gaseous phase using MEDL as illuminant has been little explored. In an interesting work developed by Xia et al. [18], an MEDL was used for the photodegradation of H_2S. They observed high removal efficiency. It is worth mentioning that they did not use any photocatalyst, so there was no problem of the deactivation of catalyst. No doubt, the photodegradation of H_2S using MEDL is promising.

In fact, the reactive oxygen species (ROS) may play a very important role during the photodegradation of H_2S with MEDL. However, the effects on the generation of ROS with MEDL in gaseous phase are not well understood. Besides, MW output power and atmosphere should affect the photodegradation process, but these effects have not been well investigated.

In this study, we examined the characteristic features of the self-made MEDL in terms of the absorbed power and spectra. The method of oxidation-extraction spectrometry (OES) with application of 1,5-diphenyl carbazide (DPCI), which has been used to determine the ROS in aqueous solution [19,20], was used to detect the ROS generated by MEDL in gaseous phase. That is, DPCI can be oxidized by ROS into 1,5-diphenyl carbazone (DPCO), which can be extracted by the mixed solution of benzene and carbon tetrachloride and show great absorbance at 563 nm wavelength. Three kinds of radical scavengers were used to determine the kinds of ROS generated by MEDL. The effects of operating parameters, including MW output power and the atmosphere on the photodegradation of H_2S were evaluated. And last, we examined the final products to explore the possible mechanism of photodegradation of H_2S.

EXPERIMENTAL SECTION

1. Materials

Benzene and carbon tetrachloride were obtained from Beijing

†To whom correspondence should be addressed.
E-mail: yujiang@mail.buct.edu.cn, yuyangbuct@126.com

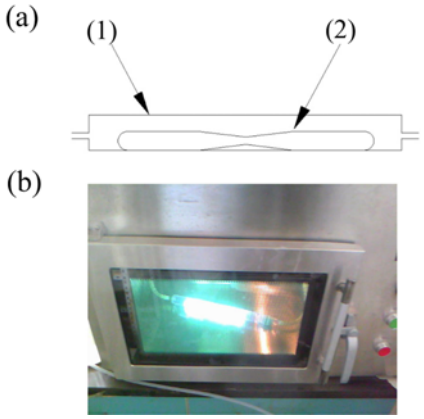

Fig. 1. (a) Configuration of the photochemical reactor: (1) quartz pipe (2) MEDL; (b) a photo of the MWP reactor with a working MEDL.

Chemical Works. L-histidine (His) and Vitamin C (VC) were purchased from Beijing Aoboxing Bio-tech Co., Ltd. Thiourea (TU) was purchased from Tianjin GuangFu technology development Co., Ltd. 1,5-diphenyl carbazide (DPCI) was obtained from Tianjin Fuchen Chemistry Works. All chemicals used were analytical grade.

2. The Microwave Photochemical (MWP) Reactor

Fig. 1(a) gives the configuration of the photochemical reactor, which consists of an MEDL and a quartz pipe. The MEDL is made of a quartz tube, filled with Hg (13.6 mg) and Ar (0.5 kPa), and sealed up at both ends. The dimension of the MEDL is 10 mm (external diameter) by 140 mm (length), but the middle of the MEDL shrank. A quartz pipe with the length of 250 mm and inner diameter of 25 mm is served as photochemical area with the MEDL in it. There is a small quartz pipe at each end of the pipe, and it is connected to a silicone tube through which the gas flows into the photochemical reactor. The photochemical reactor is placed in the MW oven (Qingdao MKW Microwave Applied Technology Co., Ltd.; power, 0-1,000 W; frequency, 2.45 GHz) comprising a microwave photochemical (MWP) reactor. The MEDL emitted UV-Vis light under a continual MW radiation. Fig. 1(b) is a photo of the MWP reactor with a working MEDL.

3. Characterization of the MEDL

In this study, the microwave output power was adjusted to 165, 330 and 660 W, respectively. The power of the MEDL was measured by the method as Zhang presented [21,22]. A beaker of water was placed in the MW oven. MW radiation could raise the temperature of the water and the beaker. The MW power absorbed by the water and the beaker can be calculated by the following equation [23]:

$$P = (c_w m_w + c_b m_b) \times \frac{\Delta T}{t} \quad (1)$$

where P is the power of MW absorbed by the water and beaker, m_w and m_b are the mass of water and beaker (water: 430.1 g, beaker: 168.5 g), c_w and c_b are the heat capacities of water and beaker (water: 4.18 J/g °C, beaker: 0.67 J/g °C), ΔT is the temperature difference (°C) between before MW radiation and after MW radiation, and t is the MW radiation time (s). The temperature of the beaker is equal to the temperature of the water in the beaker. With the MEDL in the MW field, the MW energy absorbed by the water and beaker is defined as Pa. Without the MEDL in the MW field, the MW energy absorbed by the water and beaker is defined as Pb. Pa and Pb at different MW output powers are listed in Table 1.

Table 1. MW energy absorbed by the water and beaker

MW output energy (W)	Pa[a] (W)	Pb[b] (W)	Pb-Pa (W)
165	123.05	141.39	18.34
330	235.02	267.69	32.67
660	511.12	552.96	41.84

[a]With the MEDL in the MW field
[b]Without the MEDL in the MW field

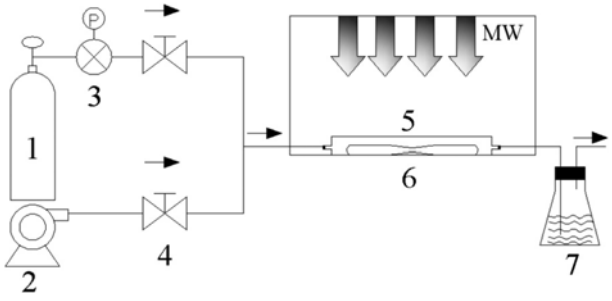

Fig. 2. Schematic diagram of the generation and trap of ROS.
1. N_2 gas cylinder
2. Air blower
3. Reducing valve
4. Mass flow controller
5. Photochemical reactor
6. MW oven
7. DPCI solution

Because some microwave energy was absorbed by the MEDL, Pa was lower than Pb. So we assume that the power of the MEDL is Pb-Pa.

The UV-Vis spectra of the MEDL were recorded by an MSB3000 spectrometer (Beijing JiKe Instrument Co., Ltd.).

4. Determination of Reactive Oxygen Species (ROS)

The experimental setup designed for the generation and trap of ROS is shown in Fig. 2. The air stream (provided by an air blower, relative humidity of air was ca. 30% at room temperature) was irradiated by MEDL at MW output powers of 165, 330 and 660 W, respectively. The N_2 stream (99.9%; Beijing Zhongkehuijie Analysis Technology Company) was irradiated by MEDL at MW output power of 660 W. Every irradiation experiment lasted for 60 min. All the above gas products were sampled into 100 mL DPCI solution (2.50 $\times 10^{-3}$ mol/L). The gas flow rate was 2 L min^{-1}. Meanwhile, the air without irradiation was also sampled into 100 mL DPCI solution at the same gas flow rate for 60 min. Then, from each sample, 10.00 mL solution was taken exactly and extracted with mixed solution of benzene and carbon tetrachloride (volume ratio=1 : 1). All extracts were then diluted to 10.0 mL with the same mixture of benzene and carbon tetrachloride solvent and their UV-Vis spectra were recorded by a spectrophotometer (Beijing Persee Co., Ltd., TU-1901).

5. Determination of the Kinds of ROS

To detect the kinds of ROS generated by MEDL, three kinds of scavengers were used to quench the different ROS. As is well known, TU can quench the hydroxyl radicals (•OH), and His can quench the singlet oxygen ($^1O_2$), while the VC can quench most kinds of ROS [24-26]. Firstly, four 25 mL DPCI stock solutions (1.00×10^2

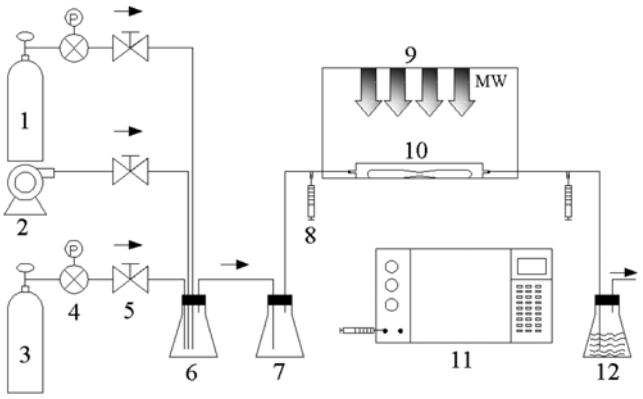

Fig. 3. Schematic diagram of photodegradation of H_2S.

1. N_2 gas cylinder
2. Air blower
3. H_2S/ N_2 gas cylinder
4. Reducing valve
5. Mass flow controller
6. Mixed gas flask
7. Surge flask
8. Glass syringe
9. MW oven
10. Photochemical reactor
11. Sulfur analyzer
12. Alkaline trap

mol/L) were added into four 100 mL volumetric flasks. Ten milliliters of stock solutions (0.05 mol/L) of His, VC and TU were added into above three volumetric flasks, respectively. All four solutions were diluted to 100 mL with distilled water and transferred into four conical flasks, respectively. Then, the air stream was irradiated by MEDL at the MW output power of 165 W for four times (60 min for each time). The gas products were sampled into the above four solutions, respectively. From each sample, 10.00 mL solution was taken exactly and extracted with mixed solution of benzene and carbon tetrachloride (volume ratio=1 : 1). Finally, all extracted solutions were diluted to 10.0 mL with the same mixed benzene-carbon tetrachloride solvent and their UV-CVis spectra were determined.

6. Photodegradation of H_2S

The experimental setup for photodegradation of H_2S, shown in Fig. 3, consists of three parts with a gas generation system, an MWP reactor, and a gas analysis system. Two kinds of gas samples were generated by mixing standard gas of H_2S (1%, N_2 as balance air, V/V; Beijing Beiwen Company) with air and N_2, respectively. The reactant gas mixture was purged into the photochemical reactor in the absence of UV-Vis illumination until a steady state was established. Then, the MW oven was powered, and the MEDL was illuminated. After a new steady state was established (after 3 min of exposure to light), a trace sulfur analyzer (Chengdu Tianyu Co., Ltd., WDL-94) was used to analyze the H_2S concentration before and after passing through the photochemical reactor. The gas residence time was 3.35 s, and the initial concentration of H_2S changed from 4 to 16 mg/m^3. They were controlled by mass flow controllers. The H_2S removal rate is calculated by the following equation:

$$H_2S \text{ removal rate } (\%) = \left(1 - \frac{\text{effluent } [H_2S]}{\text{inf luent } [H_2S]}\right) \times 100 \quad (2)$$

7. Analysis of Photodegradation Process

X-ray photoelectron spectroscopy (XPS) (Thermo Fisher Scientific, ESCALAB 250) was used to analyze S2p region of the white sediments on the inner pipe that were generated during the photodegradation of H_2S in air atmosphere.

The amount of sulfate ion product was analyzed by an ion chromatograph (IC) (Dionex, ICS-900). Sixty liters of H_2S sample gas with air/nitrogen (ca. 8.5 mg/m^3) were photodegraded, respectively. All the above gas products were introduced into 40 mL distilled water. The IC analysis was then carried out for determining the sulfate ion contents.

In addition, a gas chromatograph (GC) (Shanghai Hengping Co., Ltd., GC-1120) with thermal conductivity detector (TCD) was used to analyze H_2 production during the photodegradation of H_2S.

RESULTS AND DISCUSSION

1. Characteristics of the MEDL

As shown in Table 1, the MEDL irradiated with 165, 330 and 660 W of MW output power presented 18.3, 32.7 and 41.8 W of absorbed power, respectively. It indicates that the MEDL power increases with increasing MW output power, but there is not a linear relationship between them. The conversion process from MW energy

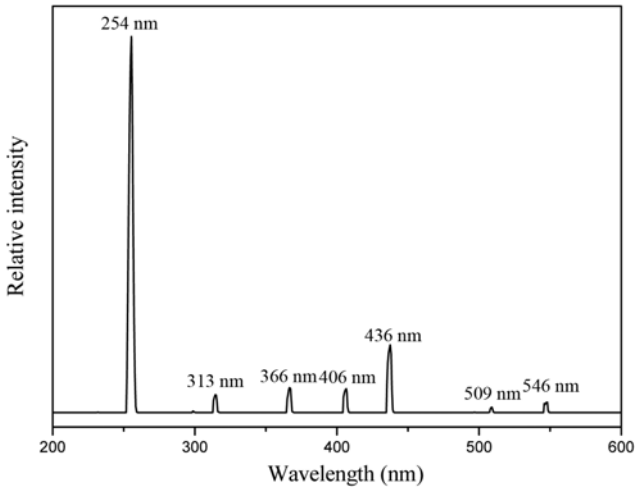

Fig. 4. UV-Vis spectroscopy of the MEDL radiated by MW at output power of 660 W.

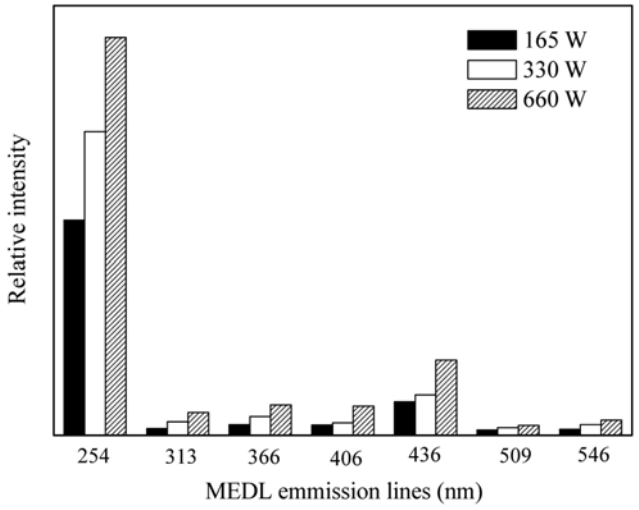

Fig. 5. Comparisons of the Hg emission line intensities with different MW output power.

to MEDL UV-Vis is complex, and the conversion efficiency is very low.

The UV-Vis spectra emitted from the MEDL under MW output power of 660 W are shown in Fig. 4. The atomic Hg emission lines for the MEDL appeared at 254, 313, 366, 406, 436, 509 and 546 nm. The MEDL showed the maximal emission at 254 nm assigned to 6^2P_1-6^2S_0 of Hg atom [18]. The energy of HS-H is 385.92 kJ mol^{-1}, corresponding to the emission line at 309 nm. Therefore, the Hg emission line at 254 nm emitted from the MEDL has enough energy to break HS-H. Fig. 5 gives the relationship of the Hg emission line intensity and MW output power. It was found that high MW output power could generate higher intensity Hg emission lines.

2. Generation of ROS by MEDL

After absorbing energetic hv emitted from MEDL, O_2/H_2O etc. molecules in air atmosphere are able to generate ROS such as •OH, $O_2^{\cdot-}$ and $^1O_2$ and so on[18]. It has been reported that the oxidation-extraction spectrometry (OES) method could be used to detect the ROS [19,20]. Because of the strong oxidation ability, the ROS can oxidize 1,5-diphenyl carbazide (DPCI) into 1,5-diphenyl carbazone (DPCO). The latter can be extracted by the mixed solution of benzene and carbon tetrachloride and show an obvious absorbance at 563 nm wavelength. Sequentially, the product and output of ROS can be detected easily.

Fig. 6 displays that the absorption peaks of DPCO in DPCI solutions after introducing irradiated air at 563 nm all show an obvious increase, compared with the corresponding one after introducing pure air. This phenomenon indicates, under UV-Vis irradiation of the MEDL, the air can generate ROS, which causes the oxidation of DPCI forming DPCO. And that the DPCO in DPCI solution after introducing irradiated N_2 does not exhibit more obvious absorbance than the corresponding one that after introducing pure air. It is clear that there is no ROS generated in N_2 atmosphere. Moreover, the absorbance of DPCO in DPCI solutions after introducing irradiated air at 563 nm increases with the increase of MW output power. It indicates that the quantities of ROS increase with the increase of MW output power.

3. The Kinds of ROS Generated During Photochemical Reaction

To explore the possible mechanisms of the photochemical process, it is important to detect the kinds of ROS. Here, three radical scavengers were used for this purpose. Through the quenching resulting from different scavengers, the kind of ROS can be judged.

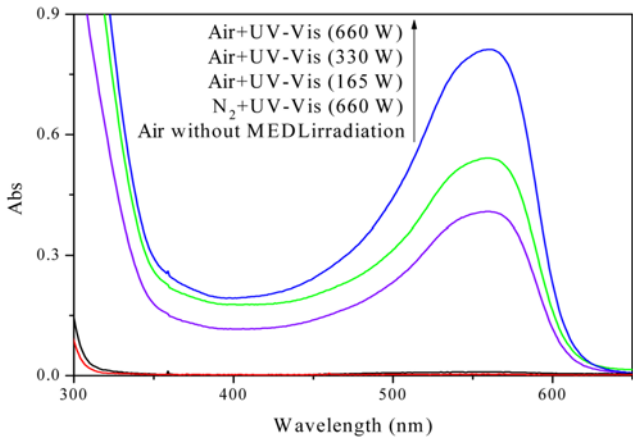

Fig. 6. UV-Vis spectra of DPCO with different reaction conditions ([DPCI]=2.50×10^{-3} mol/L).

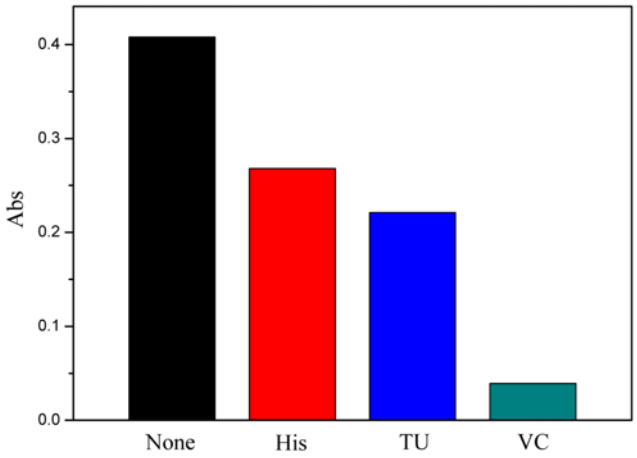

Fig. 7. Absorbance of DPCO at 563 nm as function of various quenching reagents ([DPCI]=2.50×10^{-3} mol/L, [His]=[VC]=[TU] =5.00×10^{-3} mol/L).

Fig. 7 gives the effect of introduction of scavengers on DPCO absorbance. Without any scavenger, the absorption peaks of DPCO in DPCI solutions after introducing irradiated air at 563 nm are very high. This indicates that a great amount of ROS is generated and a certain amount of DPCI is oxidized to DPCO. However, after adding quenchers, the absorbances of DPCO are weakened more or less. It implies that a number of ROS are consumed by the used scavengers, at least including $^1O_2$ and •OH.

4. Photodegradation of H_2S

Factors affecting the photodegradation process including MW output power, initial concentration of H_2S and the atmosphere were investigated. Fig. 8 displays the photodegradation of H_2S by MEDL under different conditions.

Photodegradation of H_2S under air atmosphere and nitrogen atmosphere was studied. The results are presented in line a and line d in Fig. 8, respectively. In nitrogen atmosphere, the removal efficiency

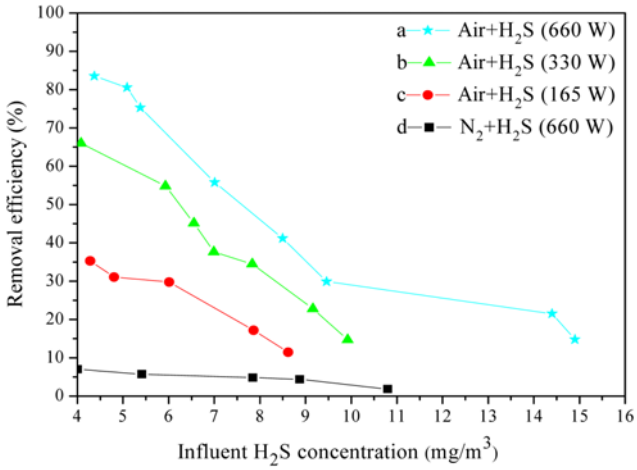

Fig. 8. Removal of H_2S in the photodegradation process under different conditions. Gas residence time in all experiments was 3.35 s.

of H_2S was lower than 7% with the initial concentration of H_2S varying from 4 mg/m^3 to 9 mg/m^3, even reaching just 2% at the initial concentration of H_2S of 10.8 mg/m^3. On the contrary, in air atmosphere with the same range of initial concentration of H_2S, the removal efficiency of H_2S was higher than 30%, even reaching up to 84% at the initial concentration of H_2S of 4.37 mg/m^3. Therefore, the photodegradation of H_2S was more effective in air atmosphere. The result of 3.2 well explains this phenomenon. It showed that the ROS was easily generated by irradiated air, while the ROS can oxidize H_2S. Thus, we believe that in nitrogen atmosphere the removal of H_2S was due to the HS-H being broken by the Hg emission line at 254 nm which could be absorbed by H_2S molecules. The removal efficiency of H_2S enhanced when in air atmosphere was mainly caused by the ROS. We consider the oxidation of H_2S by the ROS is the major mechanism in the photodegradation process under air atmosphere.

The effects of MW output power on photodegradation of H_2S are shown in lines a, b, and c in Fig. 8, respectively. The removal efficiency of H_2S increased dramatically with increasing MW output power. This was ascribed to the increase of MEDL power leading a higher light intensity to form more ROS.

In view of application, it is important to investigate the effect of the initial concentration of H_2S on the removal efficiency. The photodegradation of H_2S under the MW output power of 660 W was performed with different initial concentrations of H_2S in the range of 4 to 16 mg/m^3. The experimental results are shown in line a in Fig. 8. The removal efficiency significantly decreased with increasing the concentration of H_2S from 84% at 4.37 mg/m^3 to 15% at 14.9 mg/m^3. The reason for higher initial concentration of H_2S with lower removal efficiency can be described as follows. The number of H_2S molecules increased along with increasing initial concentration. However, the light intensity and the amount of ROS in the photochemical reactor did not increase at the fixed MW output power. Consequently, the removal efficiency became low.

5. Reaction Mechanism of Photodegradation of H_2S

The products were investigated to explore the photodegradation mechanism of H_2S. No yellow sediment was observed, which indicates that there is not any elemental sulfur produced under air or nitrogen. This implies that H_2S cannot be decomposed to element sulfur by MEDL irradiation directly.

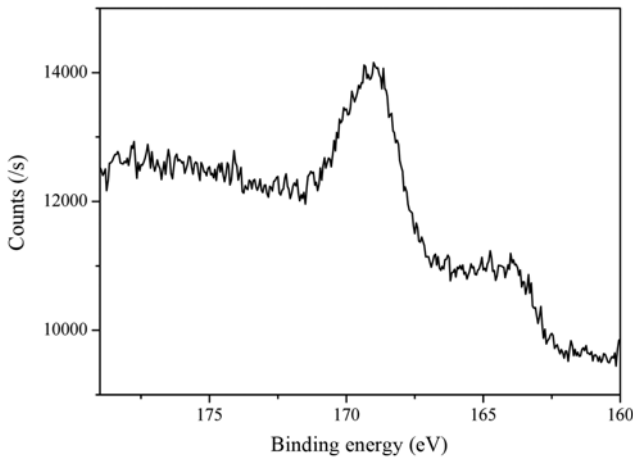

Fig. 9. X-ray photoelectron spectrum (XPS) of white sediments at S2p region during the photodegradation of H_2S in air atmosphere.

Table 2. Production concentration of SO_4^{2-} analysis via IC

Sample gas	MW output power (W)	Inlet [H_2S] (mg/m^3)	SO_4^{2-} (mg/*l*)
Pure air	660	0	0.427
H_2S+N_2	660	8.5	0.438
H_2S+air	660	8.5	11.104

But some white sediment was observed during the photodegradation of H_2S in air atmosphere. Fig. 9 shows the S2p region of XPS spectrum of white sediments on the inner pipe. The peak at 168.9 eV was due to the sulfate ion (SO_4^{2-}). The peaks of elemental sulfur (S, 164.3 eV) and sulfur dioxide (SO_2, 174.8 eV) [4] were not observed.

As shown in Table 2, the concentration of SO_4^{2-} in water that absorbed irradiated air (0.427 mg/*l*) is very small, and the SO_4^{2-} should come from water. The concentration of SO_4^{2-} in water that absorbed the products of photodegradation of H_2S with air (11.104 mg/*l*), in contrast, is very high. Thus, in air atmosphere, the H_2S that is being irradiated can generate SO_4^{2-}. The IC analysis showed that 4.63 μmol of SO_4^{2-} was formed during the photodegradation of 60 L of H_2S sample gas (in an air atmosphere). Considering that the total volume of treated H_2S and the measured H_2S removal efficiency during the sampling period were 60 L and 41%, respectively, 6.18 μmol of H_2S was eliminated at inlet H_2S concentration of 8.5 mg/m^3. Consequently, 75% of the sulfur atoms of destructed H_2S were recovered as sulfate in an air atmosphere. So the XPS and IC results suggest that the main product of photodegradation of H_2S in air atmosphere is SO_4^{2-}. On the other hand, the concentration of SO_4^{2-} in water that absorbed the products of photodegradation of H_2S with N_2 does not show an obvious increase, compared with the corresponding one that absorbed irradiated air. It indicates that the H_2S that is being irradiated in nitrogen atmosphere cannot generate SO_4^{2-}. It's interesting that the water that absorbed the products of photodegradation of H_2S with N_2 turned from colorless to yellow. It has been reported that photodegradation of sodium sulfide solutions that contain HS^- without oxygen would generate S_2^{2-} and tetrasulfide [27]. Possibly, a good amount of HS^- ions were produced by MEDL irradiation with only N_2 as carry gas, and transferred to the soluble polysulfides in aqueous solution.

Analysis of H_2 formation by the gas chromatograph shows, in air atmosphere, the formation of hydrogen was not detected during the photodegradation of H_2S process. However, the formation of hydrogen was detected during the photochemical process in nitrogen atmosphere.

Therefore, the mechanism of H_2S photodegradation can be concluded as follows:

(1) Photodegradation by MEDL irradiation in air atmosphere.

$$H_2S+hv \rightarrow HS^- + H^+$$
$$HS^- + {}^1O_2/\bullet OH \rightarrow \text{intermediates} \rightarrow SO_4^{2-}$$
$$H_2S + {}^1O_2/\bullet OH \rightarrow \text{intermediates} \rightarrow SO_4^{2-}$$

(2) Photodegradation by MEDL irradiation in nitrogen atmosphere.

$$H_2S+hv \rightarrow HS^- + H^+$$

$HS^- + hv \rightarrow HS^{-*}$

$HS^{-*} + HS^- \rightarrow \text{intermediates} \rightarrow H_2 + S_2^{2-}$

CONCLUSIONS

The power and light intensity of MEDL are dependent on MW output power. The air irradiated by MEDL could generate ROS, and the amount of ROS increases with increasing MW output power. We conclude that the removal of H_2S in air atmosphere is mainly by the ROS. In air atmosphere, sulfate is the main product of photodegradation of H_2S by MEDL irradiation. The removal efficiency of H_2S increased with increasing MW output power and decreased with increasing initial H_2S concentration.

ACKNOWLEDGEMENTS

The authors appreciate the financial support of this work by National High Technology Research and Development Program 863 (No. 2007AA06Z115) and National Natural Science Foundation of China (No.21076019).

REFERENCES

1. R. Portela, B. Sanchez, J. M. Coronado, R. Candal and S. Suarez, *Catal. Today*, **129**, 223 (2007).
2. G.-T. Jeong, G.-Y. Lee, J.-M. Cha and D.-H. Park, *Korean J. Chem. Eng.*, **25**, 118 (2008).
3. D.-R. Cho, S.-Y. Kim, D.-W. Park and P. H. Mutin, *Korean J. Chem. Eng.*, **26**, 377 (2009).
4. S. Kato, Y. Hirano, M. Iwata, T. Sano, K. Takeuchi and S. Matsuzawa, *Appl. Catal. B: Environ.*, **57**, 109 (2005).
5. M. P. Chenar, H. Savoji, M. Soltanieh, T. Matsuura and S. Tabe, *Korean J. Chem. Eng.*, **28**, 902 (2011).
6. S.-H. Kim, I. H. Kim, W. J. Lee and J.-H. Lee, *Korean J. Chem. Eng.*, **25**, 1131 (2008).
7. M. C. Canela, R. M. Alberici and W. F. Jardim, *J. Photochem. Photobiol. A: Chem.*, **112**, 73 (1998).
8. J. S. Jang, W. Li, S. H. Oh and J. S. Lee, *Chem. Phys. Lett.*, **425**, 278 (2006).
9. J. S. Jang, H. Gyu Kim, P. H. Borse and J. S. Lee, *Int. J. Hydrog. Energy*, **32**, 4786 (2007).
10. S. Kataoka, E. Lee, M. I. Tejedor-Tejedor and M. A. Anderson, *Appl. Catal. B: Environ.*, **61**, 159 (2005).
11. X. Zhang, Y. Wang and G. Li, *J. Mol. Catal. A: Chem.*, **237**, 199 (2005).
12. J. Hong, C. Sun, S.-G. Yang and Y.-Z. Liu, *J. Hazard. Mater.*, **133**, 162 (2006).
13. Z. Gao, S. Yang, N. Ta and C. Sun, *J. Hazard. Mater.*, **145**, 424 (2007).
14. J. Hong, N. Ta, S.-g. Yang, Y.-z. Liu and C. Sun, *Desalination*, **214**, 62 (2007).
15. V. Církva, H. Žabová and M. Hájek, *J. Photochem. Photobiol. A: Chem.*, **198**, 13 (2008).
16. J. r. Literák and P. Klán, *J. Photochem. Photobiol. A: Chem.*, **137**, 29 (2000).
17. P. Klán, M. Hájek and V.r. Církva, *J. Photochem. Photobiol. A: Chem.*, **140**, 185 (2001).
18. L.-Y. Xia, D.-H. Gu, J. Tan, W.-B. Dong and H.-Q. Hou, *Chemosphere*, **71**, 1774 (2008).
19. J. Wang, Y. Guo, J. Gao, X. Jin, Z. Wang, B. Wang, K. Li and Y. Li, *Ultrason. Sonochem.*, **18**, 1028 (2011).
20. Z. Zhang, Y. Xu, X. Ma, F. Li, D. Liu, Z. Chen, F. Zhang and D. D. Dionysiou, *J. Hazard. Mater.*, **209-210**, 271 (2012).
21. X. Zhang, G. Li and Y. Wang, *Dyes Pigm.*, **74**, 536 (2007).
22. X. Zhang, Y. Wang, G. Li and J. Qu, *J. Hazard. Mater.*, **134**, 183 (2006).
23. D.-H. Han, S.-Y. Cha and H.-Y. Yang, *Water Res.*, **38**, 2782 (2004).
24. S.-i. Umemura, N. Yumita, K. Umemura and R. Nishigaki, *Cancer Chemoth. Pharm.*, **43**, 389 (1999).
25. R. Dai, R. Shoemaker, D. Farrens, M. J. Han, C. S. Kim and P.-S. Song, *J. Nat. Prod.*, **55**, 1241 (1992).
26. S. Sachdev and K. J. A. Davies, *Free Radical Biol. Med.*, **44**, 215 (2008).
27. C. A. Linkous, C. Huang and J. R. Fowler, *J. Photochem. Photobiol. A: Chem.*, **168**, 153 (2004).